Appl Microbiol Biotechnol (2011) 90:117–126
DOI 10.1007/s00253-010-3029-x

BIOTECHNOLOGICALLY RELEVANT ENZYMES AND PROTEINS

Identification and characterization of 4-hexylbenzoic acid and 4-nonyloxybenzoic acid as substrates of CYP102A1

Rama Krishna Gudiminchi · Martha Sophia Smit

Received: 3 October 2010 / Revised: 18 November 2010 / Accepted: 23 November 2010 / Published online: 16 December 2010

Abstract CYP102A1 is an efficient medium- to long-chain fatty acid hydroxylase that is able to accept a wide range of non-natural substrates which bear no resemblance to the natural ones. 4-Hexylbenzoic acid (HBA) and 4-nonyloxybenzoic acid (NOBA) were identified as CYP102A1 substrates via screening studies using the BD Oxygen Biosensor System. Spectroscopic binding studies showed that these two substrates bind in the active site of CYP102A1 with K_d values of 2.6±0.1 μM for HBA and 1.9±0.2 μM for NOBA. NADPH consumption rates in the presence of HBA and NOBA were 45±1 min^{-1} and 61±1 min^{-1}, respectively. The coupling efficiency for NADPH was 57% for NOBA, while it was 77% for HBA. During whole-cell biotransformations, HBA was converted into ω−1- and ω−2-hydroxyhexylbenzoic acid, whereas NOBA was oxidized to ω−2-hydroxynonyloxybenzoic acid and ω−2,ω−4-dihydroxynonyloxybenzoic acid. HBA was used as a fatty acid mimic to compare whole-cell biotransformations with cell-free extracts. Whole-cell biotransformations carried out in a biphasic system resulted in 86% conversion of 5 mM HBA, producing 3.8 mM ω−2- and 0.5 mM ω−1-hydroxyhexylbenzoic acid in 4 h with a turnover number of 4.1 min^{-1}, whereas 100% conversion of 5 mM HBA was obtained in 1 h with crude cell extracts and a cofactor regeneration system, giving a turnover number of 10.5 min^{-1}.

Keywords CYP102A1 · P450 BM-3 · Substrate screening · Fluorescence-based oxygen consumption · 4-Hexylbenzoic acid · 4-Nonyloxybenzoic acid · Whole-cell biotransformation

South African DST-NRF Centre of Excellence in Catalysis, c*change

R. K. Gudiminchi · M. S. Smit (✉)
Department of Microbial, Biochemical and Food Biotechnology,
University of the Free State,
P.O. Box 339, Bloemfontein 9300, South Africa
e-mail: smitms@ufs.ac.za

Introduction

CYP102A1, also known as P450 BM-3, is a catalytically self-sufficient NADPH-dependent cytochrome P450 monooxygenase that is classified as a class II P450 enzyme (Ravichandran et al. 1993). It is a water-soluble fusion protein (M_r 118 kDa) that consists of a heme domain and a FAD/FMN reductase domain in a single polypeptide chain. It was isolated from *Bacillus megaterium* (Narhi and Fulco 1982), and cloned and functionally expressed in various *Escherichia coli* strains (Wen and Fulco 1987). CYP102A1 catalyzes the epoxidation of unsaturated fatty acids and the hydroxylation of medium- to long-chain saturated fatty acids at sub-terminal positions (Graham-Lorence et al. 1997). This enzyme is relatively stable and belongs to the most active P450s described to date. It hydroxylates fatty acids with turnover rates of more than 1,000 min^{-1} (Boddupalli et al. 1990; Ost et al. 2000).

CYP102A1 has a high degree of plasticity as it has been modified to accept a wide range of non-natural substrates which do not bear any resemblance to the natural ones (Eiben et al. 2006). The wild-type CYP102A1 can hydroxylate short-chain alkylbenzenes at the benzylic position (Whitehouse et al. 2008b). We wanted to establish whether CYP102A1 can accept longer-chain (C8 to C16) alkylbenzenes, alkylbenzoic acids, and alkyloxybenzoic acids as substrates. These compounds resemble long-chain alkanes and fatty acids, but are not as often completely degraded by β-oxidation. This makes them attractive model compounds for studying aspects of alkane and fatty acid hydroxylation using whole cells of microorganisms with intact β-oxidation. The UV absorbance of these compounds and their hydroxy products is also advantageous for tracking the utilization of substrates and the formation of products using thin layer chromatography. Additionally, hydroxylated products from alkylbenzoic acids and alkoxybenzoic acids might be interesting monomers for

the synthesis of novel polymers. To our knowledge, there are no reports where alkylbenzoic acids and alkyloxybenzoic acids have been demonstrated as potential CYP102A1 substrates.

4-Hexylbenzoic acid (HBA) and 4-nonyloxybenzoic acid (NOBA) were identified as substrates of CYP102A1 via screening studies of medium- to long-chain alkylbenzenes, alkylbenzoic acids, and alkyloxybenzoic acids using the BD Oxygen Biosensor System, which was used during the screening of potential substrates and ligands for plant P450s (Olry et al. 2007). Oxidations of HBA and NOBA were studied in vivo and in vitro, and sub-terminally hydroxylated products were recovered from the reaction mixtures without any further degradation. Binding constants and coupling efficiencies were also determined for each substrate.

Materials and methods

Chemicals, bacterial strains, and plasmids

Chemicals were obtained from Sigma-Aldrich, Merck, or Acros Organics. pET28a-*CYP102A1*, kindly provided by Prof. Vlada B. Urlacher (then at Institute of Technical Biochemistry, Stuttgart University, Germany, currently at the Institute of Biochemistry, Heinrich-Heine-University, Düsseldorf) was transformed into competent *E. coli* BL21 (DE3) cells for expression. Glycerol stock was prepared from a single colony and stored at −80 °C.

CYP102A1 expression and purification

Five milliliters of LB medium (Sambrook et al. 1989) supplemented with 30 μg mL^{-1} kanamycin was inoculated with 20 μL *E. coli* BL21(DE3) glycerol stock and incubated overnight at 30 °C. One milliliter of this culture was added to 50 mL TB medium (Pflug et al. 2007) supplemented with kanamycin (30 μg mL^{-1}) in a 250-mL flask and incubated at 37 °C to OD_{578} 0.8–1.1. Expression was induced with 0.5 mM isopropyl-β-D-thiogalactopyranoside (IPTG). The culture was supplemented with 1 mM δ-aminolevulinic acid and incubated at 30 °C for 10 h. The cells were harvested by centrifugation (6,000×*g*, 10 min, 4 °C) and the pellet was resuspended in a ratio of 1:3 wet weight per volume (g mL^{-1}) in potassium phosphate buffer (50 mM, pH 7.4) containing 0.5 mM dithiothreitol (DTT) and 1 mM ethylenediaminetetraacetic acid (EDTA). The cells were lysed using a Constant Cell Disruption System (Constant Systems Ltd, UK; 32.5 kpsi) and the membrane and soluble fractions were separated by centrifugation (20,000×*g*, 30 min, 4 °C). CYP102A1 was purified from the soluble fraction using a His-Trap column (Amersham) and eluted in potassium phosphate buffer (50 mM, pH 7.4) containing 500 mM NaCl, using a linear imidazole gradient (20–500 mM) with a flow rate of 5 mL min^{-1}. This was followed by size-exclusion chromatography using a Sephacryl 200 column (Sigma) and elution in potassium phosphate buffer (50 mM, pH 7.4) containing 50 mM NaCl. The protein purity was analyzed by SDS–PAGE.

Quantification of CYP102A1

CYP102A1 content was quantified using CO-difference spectra (Omura and Sato 1964), carried out in F8 Maxisorp Nunc-Immuno™ Modules (Nunc A/s, Denmark). Samples of 200 μL were added into wells in two different microtiter strips (Choi et al. 2003) and one well of each sample was saturated with carbon monoxide by exposure to carbon monoxide flow for 5 min. The samples in both microtiter strips were reduced by adding a few grains of sodium dithionite, followed by shaking for 10 s. The spectrum between 350 nm and 600 nm was recorded using a Spectramax M2 Microtiter Plate Reader (Molecular Devices Corporation, USA), with the well not saturated with carbon monoxide serving as the reference, until a stable $A_{450–490}$ difference was obtained (usually within 10 min of sodium dithionite addition). The $A_{450–490}$ difference was corrected for a pathlength of 1 cm and the P450 concentration was calculated using an extinction coefficient of 91 $mM^{-1}cm^{-1}$.

Substrate screening studies

Screening studies of potential CYP102A1 substrates were carried out using the BD Oxygen Biosensor System. Reaction mixtures (190 μL) containing 450 μM NADPH, 3 mM glucose-6-phosphate, 0.4 U glucose-6-phosphate dehydrogenase, and 250 μM substrate (free acid in the case of organic acids) dissolved in DMSO (0.5% v/v final concentration in the reaction mixture) were pre-incubated at 27 °C for 5 min. The reaction was initiated by the addition of 10 μL soluble fraction, resulting in a final CYP102A1 concentration of 400–600 nM. The change in fluorescence in each well at 27 °C was recorded every 30 s for 2 h using excitation and emission wavelengths of 486 nm and 620 nm, respectively. The fluorescence value of each well was normalized using the fluorescence prior to enzyme addition, and the fold increase in fluorescence, corresponding to the oxygen consumed, was estimated after 1 min and plotted against time (Olry et al. 2007). The slopes were calculated to compare oxygen consumption rates in the presence of different compounds (Rolo et al. 2009).

NADPH consumption rate and coupling efficiency

The enzyme activity towards different compounds was measured using an NADPH oxidation assay. A 1-mL

reaction mixture containing 0.3 μM purified CYP102A1, 150 μM substrate (free acid in the case of organic acids) dissolved in DMSO (0.5% v/v final concentration in the reaction mixture), and potassium phosphate buffer (50 mM, pH 7.4) was pre-incubated for 5 min at 27 °C. The reaction was initiated by the addition of 300 μM NADPH. Aliquots of 200 μL were transferred into a 96-well plate and the NADPH consumption was monitored at 340 nm. NADPH consumption rates were determined from the slopes obtained after the initial 30 s of the reaction and the NADPH consumed was calculated using a standard curve generated using different NADPH concentrations. Coupling efficiencies were determined using a similar reaction setup, with the exception of an NADPH concentration of 100 μM. The reactions were monitored until all the NADPH was consumed and the substrate consumption and product formation was analyzed using GC. Authentic standards were not available for the quantification of the products; therefore, the concentrations of substrates utilized were calculated from the GC peak area ratios and related to the added amount of NADPH to determine the coupling efficiencies (Eiben 2007).

Substrate-binding studies

Substrate-binding studies (Noble et al. 1999) were carried out using 1 μM purified enzyme in 1 mL potassium phosphate buffer (50 mM, pH 7.4), with 1-cm quartz cuvettes. A concentrated solution of substrate (free acid) in DMSO was added to produce a final substrate concentration of between 0.5 μM and 300 μM. The total volume of substrate added was kept below 1.5% of the initial volume in the cuvette. Spectral changes between 350 nm and 650 nm were recorded using a Varian UV–Vis spectrophotometer (Cary 300Bio UV–Vis spectrophotometer) and the binding constants (K_d) were determined for each substrate by following the shift in the absorbance maximum from 420 nm to 389 nm, as a result of a shift in the state of the heme-iron from low-spin to high-spin upon substrate-induced replacement of the sixth ligand (water) of the heme iron in the substrate-free state (Modi et al. 1995).

Biotransformations

The biocatalytic efficiency towards substrates was determined using whole cells and soluble fractions of crude cell extracts. In the case of the whole cells, the 16-h post-induction cell pellet of 50 mL culture broth (~1 g wet cell weight) was resuspended in 5 mL potassium phosphate buffer (50 mM, pH 8.0) containing $FeSO_4 \cdot 7H_2O$ (100 μg mL^{-1}) and 0.8% glycerol (Fujii et al. 2006). Reaction mixtures of 2 mL, defined as the biotransformation reaction mixture (BRM), were set up and comprised 8 μM CYP102A1 (in whole cells or soluble fractions), 5 mM substrate (free acid) dissolved in DMSO (2% v/v final DMSO concentration in the reaction mixture), water, and different volumes of potassium phosphate buffer (1 M, pH 8.0) so as to generate final buffer concentrations of 50 mM, 100 mM, or 200 mM. In the case of the whole cells, 25 mM glucose was included in the BRM, whereas in the case of the soluble fractions, 6.5 U mL^{-1} glucose-6-phosphate dehydrogenase, 8 mM glucose-6-phosphate, and 900 μM NADPH was included in the BRM. A biphasic system was also set up

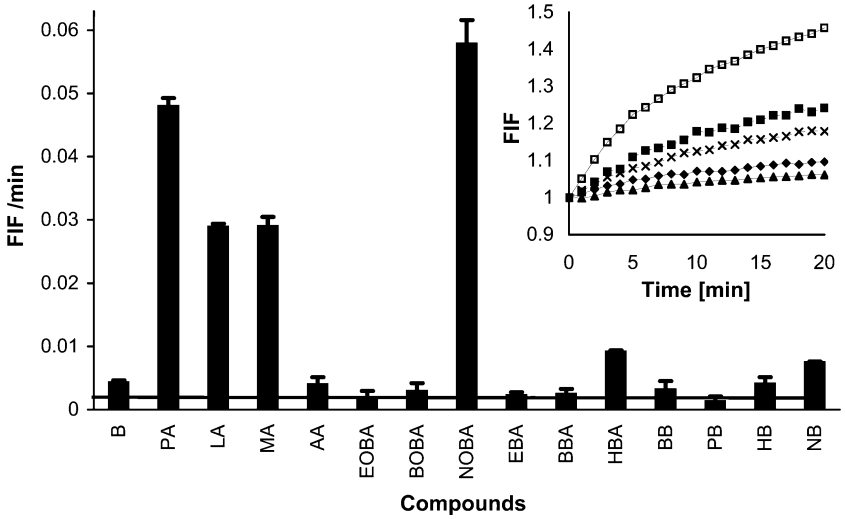

Fig. 1 Rate of fold increase in fluorescence (*FIF*) as measured using the BD Oxygen Biosensor System in the absence of substrate (*B*) and in the presence of palmitic acid (*PA*), lauric acid (*LA*), myristic acid (*MA*), 4-anisic acid (*AA*), 4-ethoxybenzoic acid (*EOBA*), 4-butoxybenzoic acid (*BOBA*), 4-nonyloxybenzoic acid (*NOBA*), 4-ethylbenzoic acid (*EBA*), 4-butylbenzoic acid (*BBA*), 4-hexylbenzoic acid (*HBA*), butylbenzene (*BB*), pentylbenzene (*PB*), hexylbenzene (*HB*), and nonylbenzene (*NB*). Values were obtained from the average of triplicates. Standard deviations are indicated. *Inset*: fold increase in fluorescence (*FIF*) in the presence of palmitic acid (*solid squares*), 4-butylbenzoic acid (*solid triangles*), 4-hexylbenzoic acid (*crosses*), and 4-nonyloxybenzoic acid (*open squares*), and in the absence of substrate (*solid diamonds*)

by adding 400 μL hexadecane, containing substrate (5 mM final concentration in reaction mixture), to 2 mL of whole-cell BRM containing potassium phosphate buffer (200 mM, pH 8.0), DMSO (2% v/v) and no substrate. The reaction mixtures were transferred to 40-mL sterile amber screw-cap vials and incubated on a shaker at 30 °C. Vials were taken out at specific time intervals and the residual CYP102A1 content was quantified.

Sample extractions and product analyses

HCl (140 μL, 5 M) was added to a 1-mL reaction sample and extracted twice with 500 μL ethyl acetate containing 0.1 mM myristic acid as internal standard (Smit et al. 2005). The combined organic phases were dried under a gentle stream of nitrogen and the residual sample was methylated for GC analysis (Barrow and Taylor 1987) by the addition of 200 μL trimethyl sulfonium hydroxide, followed by incubation at room temperature for 1 h. GC analysis was carried out using a Hewlett Packard 5890 Series II gas chromatograph equipped with a flame ionization detector and a Supelco wax 10 CB column measuring 30 m×0.53 mm. The temperature program used was as follows: 150 °C, 5 min isotherm, ramp of 10 °C min^{-1} to 250 °C, 10 min isotherm. The inlet temperature was 200 °C, the flow of hydrogen (carrier gas) through the column was 6 mL min^{-1}, and the sample volume was 1 μL. Product concentrations were calculated using a standard curve of respective substrates, assuming that the signal intensities of the substrates are similar to those of the respective hydroxylated products.

Samples for GC–MS analysis were methylated and then dried under a nitrogen stream. The residue was dissolved in 100 μL pyridine and 100 μL bis(trimethylsilyl)trifluoroacetamide (BSTFA) was added, followed by incubation at room temperature for 40 min to yield the trimethylsilylated product (Barrow and Taylor 1987). The sample was dried under a nitrogen stream and the residue was dissolved in 20–50 μL ethyl acetate. GC–MS analysis was carried out using a Finnigan Trace GC ultra chromatograph, with a ZB-WAX column measuring 30 m×0.25 mm, with helium (carrier gas) at a flow rate of 1 mL min^{-1}, using the above-mentioned temperature program.

Results

Substrate screening studies

CYP102A1 was over-expressed in *E. coli* BL21(DE3) as a soluble protein and the active P450 was quantified using CO-difference spectra. Several alkylbenzenes, alkylbenzoic acids, and alkyloxybenzoic acids with alkyl-chain lengths of one to nine carbons were screened, along with palmitic acid, lauric acid, and myristic acid, which are known CYP102A1 substrates. The screening studies were carried out using the BD Oxygen Biosensor System, which consists of a 96-well plate that has an oxygen-sensitive fluorophore embedded in a silicone matrix at the bottom of each well (Wodnicka et al. 2000). The presence of oxygen in the matrix suppresses the fluorophore, but as the concentration of oxygen is depleted by the enzymatic reaction, the fluorescent signal increases. The initial screening studies were carried out using whole cells, but high cellular respiration resulted in high increases in fluorescence, corresponding to high levels of oxygen consumption in the absence of substrate. Soluble fractions of cell-free extracts containing active CYP102A1 were therefore used instead and were diluted so as to maintain a CYP102A1 concentration of 400–600 nM per well, which resulted in only a low background fluorescence increase in the absence of substrate. Experiments were also performed without the addition of NADPH, but when soluble fractions

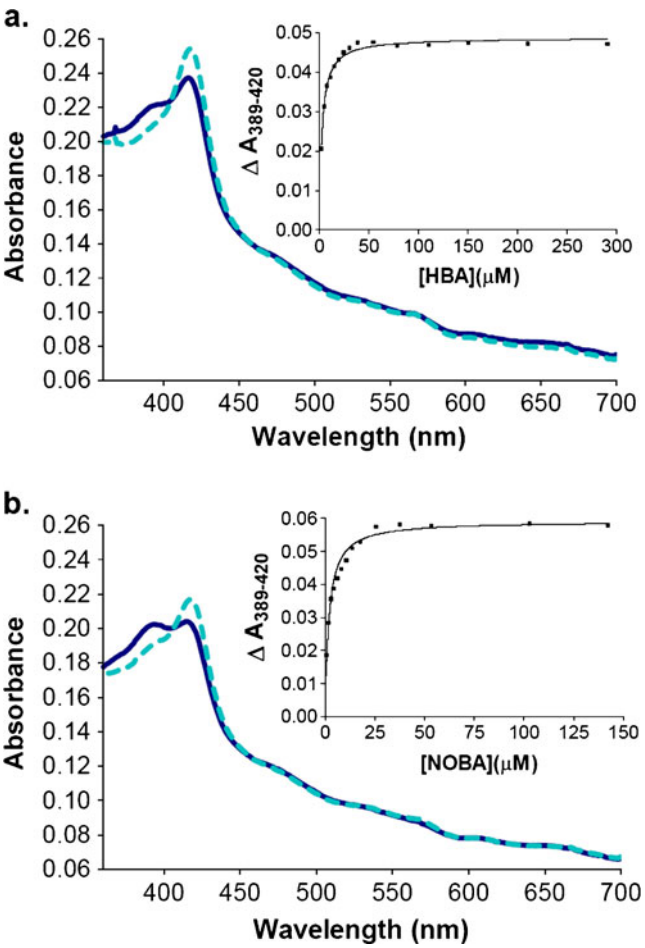

Fig. 2 Type I binding spectra obtained from the titration of CYP102A1 (1 μM) with **a** HBA (*light dashed line* no substrate; *dark solid line* 4.5 μM) and **b** NOBA (*light dashed line* no substrate; *dark solid line* 1.5 μM) showing isobestic points at 405 nm for HBA and 407 nm for NOBA. *Insets* absorption difference between 389 nm and 420 nm, plotted against substrate concentrations

of fresh extracts were used, relatively large increases in fluorescence were obtained because of the presence of endogenous NADPH. Therefore, only reaction mixture without substrate was used as a blank to determine the background oxygen consumption. The rates of the fold increase in fluorescence were calculated from the initial slopes (Rolo et al. 2009), which were obtained within 1 to 10 min after the initiation of the reaction (Fig. 1). These were used to identify the compounds which might serve as substrates. A significant increase in fluorescence was obtained in the presence of palmitic acid, lauric acid, and myristic acid, the natural substrates of CYP102A1, indicating oxygen consumption. An increase in fluorescence, comparable to that of the wells containing these natural substrates, was obtained in the presence of NOBA, while HBA gave a response that was approximately double the response observed in the absence of substrates. The increase in fluorescence in the presence of nonylbenzene was higher than in the absence of substrates and only slightly lower than with HBA, but this result was not supported by substrate confirmation studies (data not shown).

Substrate-binding spectra and NADPH consumption

Type I binding spectra were obtained when purified CYP102A1 (1 μM) was titrated with HBA and NOBA (Fig. 2). This provided evidence of the affinity of the enzyme for HBA and NOBA and confirmed that these compounds are CYP102A1 substrates. Apparent binding constants (K_d) were calculated by plotting the values of the absorbance difference, $A_{389–420}$, against substrate concentrations (Noble et al. 1999; Huang et al. 2007). The binding constants of CYP102A1 with HBA and NOBA were 2.6±0.1 μM and 1.9±0.2 μM, respectively (Table 1).

The NADPH consumption rate was 45±1 min^{-1} in the presence of HBA and 61±1 min^{-1} in the presence of NOBA. With a limited NADPH concentration of 100 μM and low HBA and NOBA concentrations of only 150 μM, only one major product peak for each of these substrates was observed in the GC analyses of methylated samples. The coupling efficiencies were therefore calculated with respect to the percent substrate consumed after the complete utilization of NADPH. The coupling efficiency of CYP102A1 was 77% in the presence of HBA and 57% in the presence of NOBA (Table 1).

Identification of products

GC–MS analysis of methylated and silylated extracts from whole-cell biotransformations was used to determine the positions at which the substrates were hydroxylated. Fragmentation of the methylated and silylated products from HBA indicated that it was mainly hydroxylated at the ω−2 position, forming ω−2-hydroxyhexylbenzoic acid as the major product, or at the ω−1 position, forming ω−1-hydroxyhexylbenzoic acid as the minor product (Fig. 3). Both of the products formed from HBA could also be detected with GC analysis of samples that were only methylated, and quantitative analysis of product formation with GC analysis gave satisfactory results when it was assumed that the response for the products was the same as for the substrate (i.e., the sum of the relative areas for HBA and the products remained constant over time). The ratio of ω−2:ω−1 hydroxylation was ca. 7:1 and remained constant over time. This ratio was also not affected by biotransformation conditions when these were varied in later experiments.

Fragmentation of the methylated and silylated products from NOBA indicated that NOBA was also initially hydroxylated at the ω−2 position, forming ω−2-hydroxynonyloxybenzoic acid as the major product (Fig. 4). At later stages of the reaction, this product was also hydroxylated at the ω−4 position, resulting in the formation of

Table 1 Activity, coupling efficiency, and binding constants of wild-type CYP102A1 with different substrates

Substrate	[NADPH] nmol min^{-1} $nmol^{-1}$ of CYP102A1	Coupling efficiency (%)	K_d value (μM)	Reference(s)
4-Hexylbenzoic acid	45±1	77	2.6±0.1	Present study
4-Nonyloxybenzoic acid	61±1	57	1.9±0.2	Present study
Lauric acid	2,777	52	270	Whitehouse et al. (2009) Huang et al. (2007)
Myristic acid	4,835	88	6.9	Girvan et al. (2004) Cryle et al. (2007)
Palmitic acid	4,590	93	11.3	Girvan et al. (2004) Cryle et al. (2007)
Propylbenzene	866	71	73.5	Li et al. (2001) Whitehouse et al. (2008a)
4,6,8 Trimethyldecane-2-ol	59.5	83	>200	Budde et al. (2006)
4,6,8 Trimethyldecanoic acid	150.7	23	ND	Budde et al. (2006)

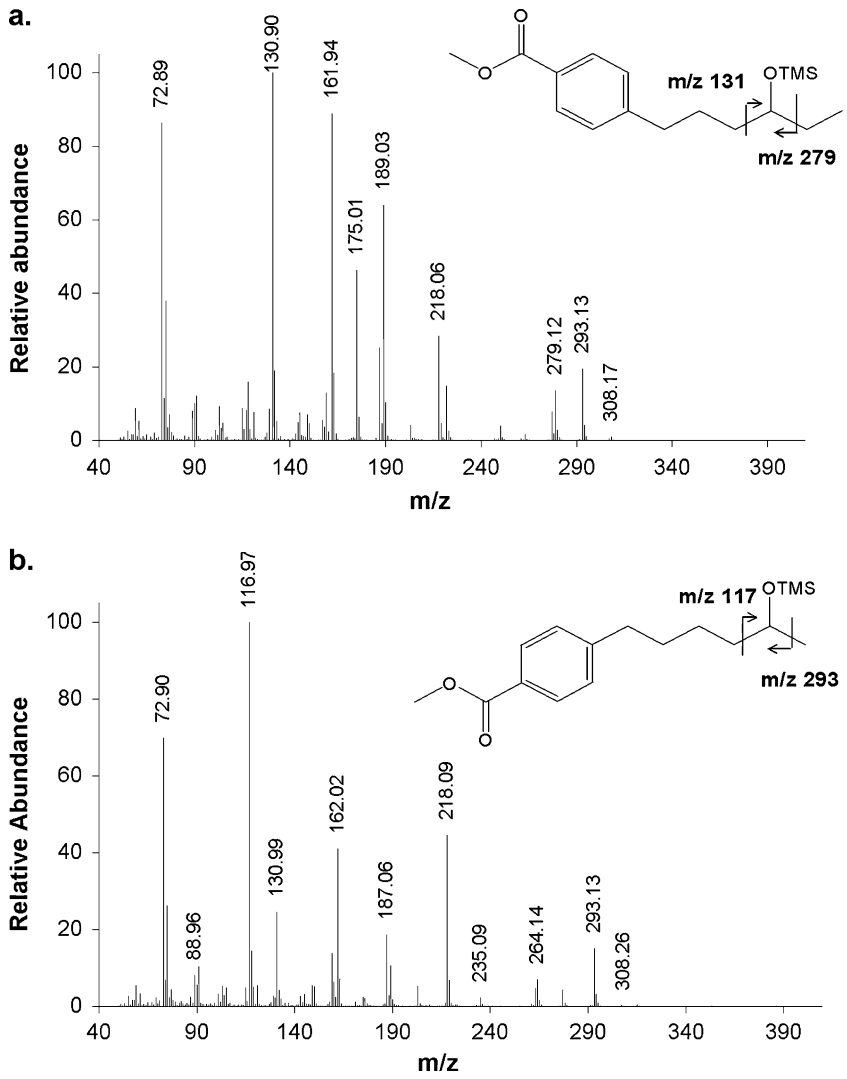

Fig. 3 GC–MS spectra of the methylated and trimethylsilylated derivatives of **a** ω−2-hydroxyhexylbenzoic acid and **b** ω−1-hydroxyhexylbenzoic acid showing the expected molecular ion at *m/z* 308 as well as M^+-15 at *m/z* 293

ω−2,ω−4-dihydroxynonyloxybenzoic acid. It was possible to detect the monohydroxylated product with GC analysis of only methylated extracts, but the dihydroxylated product could only be detected if the samples were methylated and silylated. It was not possible to accurately quantify the products formed from NOBA using GC analysis since the sum of the relative areas of NOBA and its products was not constant over time. TLC also indicated that more over-oxidized products were formed which were not detected using GC analysis. It is also possible that all of the products were not extracted. HPLC analysis of filtered reaction mixtures from NOBA biotransformations is an option that should be investigated in the future.

Stability of CYP102A1 during whole-cell biotransformations of HBA and NOBA

The substrate concentration used for all of the biotransformation experiments was 5 mM and the CYP102A1 concentration was 8 μM. The initial biotransformations were conducted using whole cells in 50 mM potassium phosphate buffer (pH 7.4). The residual P450 activity was determined after 4 h and 19 h using CO-difference spectra. After 19 h, a decrease in catalytically active CYP102A1 was observed when compared to CYP102A1 in the absence of substrate. This was evident from a decrease in the P450 peak and the formation of a P420 peak, indicating the formation of inactive P420 species (Fig. 5). In the presence of NOBA, 82% of the P450 was still active, whereas in the presence of HBA, only 16% of the P450 remained active. In these initial experiments, only 15% of the HBA was converted to products within 19 h, while the conversion of NOBA was at least 25%. As the insolubility of NOBA complicated sampling and the quantification of NOBA and its products, quantification of further biotransformation experiments was only done for HBA. Since HBA consumption leveled off between 4 h and 19 h and no P420 peak was observed after 4 h, the reaction time was reduced

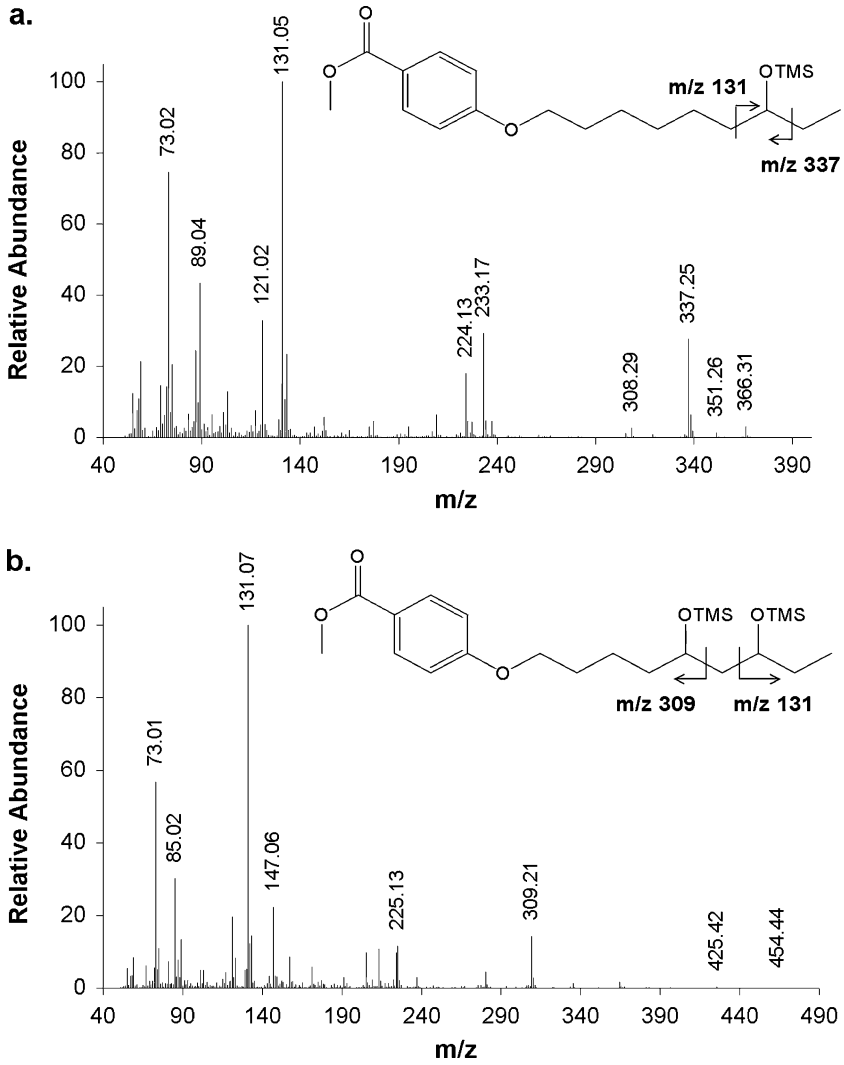

Fig. 4 GC–MS spectra of the methylated and trimethylsilylated derivatives of **a** ω−2-hydroxynonyloxybenzoic acid and **b** ω−2,ω−4-dihydroxynonyloxybenzoic acid showing the expected molecular ions at *m/z* 366 and *m/z* 454, respectively

to 4 h for the rest of the biotransformation experiments with HBA.

Effect of substrate availability on whole-cell biotransformation of HBA

The biotransformation results obtained with HBA are summarized in Table 2. In order to investigate factors limiting whole-cell biotransformation, the first parameter that was investigated was substrate availability. Tsotsou et al. (2002) reported an increase in the permeability of *E. coli* cells by partial lysis using 100 mM potassium phosphate buffer at pH 8.0. Based on these results, whole-cell biotransformations of HBA were conducted using 50 mM, 100 mM, and 200 mM potassium phosphate buffer at pH 8.0. Whole-cell CO-difference spectra done after 4 h showed that the change in pH and the variation in buffer concentration did not affect the stability of CYP102A1 during the 4-h reaction. Increasing the pH from 7.4 to 8.0 resulted in the substrate conversion after 4 h doubling from

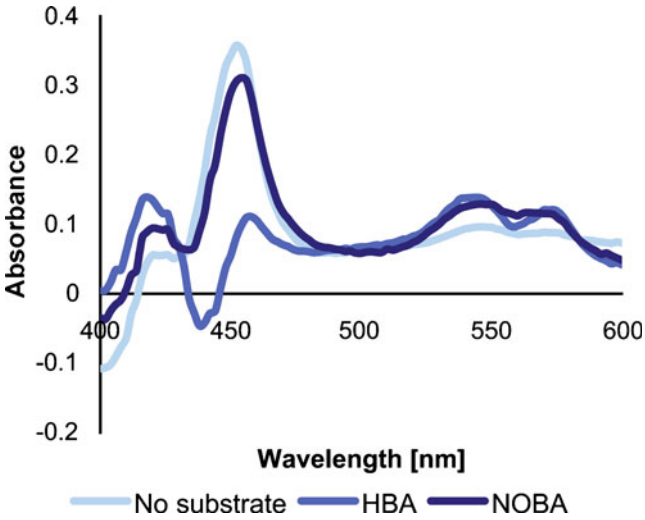

Fig. 5 Residual intact CYP102A1 in whole cells in the absence of substrate (*light line*) and in the presence of HBA (*medium line*) or NOBA (*dark line*) after 19 h of whole-cell biotransformation

Table 2 Summary of biotransformation results obtained with HBA

Reaction	pH	Buffer concentration (mM)	Total product formed after 4 h (mM)	Product formation rate[a] ($mM\,min^{-1}$)	Specific rate[a] (min^{-1})
WC_Aq	7.4	50	0.6	0.004	0.5
WC_Aq	8.0	50	1.1	0.006	0.7
WC_Aq	8.0	100	2.4	0.010	1.2
WC_Aq	8.0	200	3.0	0.017	2.1
WC_Biph	8.0	200	4.3	0.032	4.1
Sol_Aq	8.0	50	5.0	0.083	10.4

WC whole cells, *Sol* soluble fractions of cell-free extracts, *Aq* aqueous phase only, *Biph* biphasic system

[a] Calculated from conversion after 1 h

12% to 22%. Increasing the buffer concentration to 100 mM and 200 mM further increased the substrate conversion to 48% and 60%, respectively.

Whole cells expressing CYP102A1 and cell-free extracts containing CYP102A1 have been studied in biphasic systems to increase the turnover numbers and product yields (Maurer et al. 2005; Mouri et al. 2006). In order to study the effect of biphasic systems on the regioselective hydroxylation of HBA by CYP102A1 and the acceleration of the reaction rate, whole-cell biotransformation studies were conducted using hexadecane as an organic phase and 200 mM potassium phosphate buffer (pH 8.0) as an aqueous phase (Sowden et al. 2005). The total substrate conversion was increased to 86% after a 4-h reaction with the ω−2:ω−1 hydroxylation ratio remaining 7:1. Thus, with the whole-cell biotransformations, the maximum product formed from 5 mM HBA was 3.8 mM ω−2- and 0.5 mM ω−1-hydroxyhexylbenzoic acid.

To further evaluate the diffusion barrier and the limitation of intracellular NADPH concentration, biotransformations were conducted under similar experimental conditions using the soluble fraction of crude cell extracts in 50 mM potassium phosphate buffer (pH 8.0) with cofactor regeneration by glucose-6-phosphate dehydrogenase. In this case, 100% of the substrate was utilized within 1 h. The product ratio remained unchanged. Thus, the maximum specific hydroxylation rate obtained with whole cells was 4.1 min^{-1} when 200 mM potassium phosphate buffer (pH 8.0) was used in a biphasic system with hexadecane, while the maximum specific hydroxylation rate obtained with crude cell-free extract was 10.4 min^{-1}.

Discussion

Oxygen consumption measured using the fluorescence-based BD Oxygen Biosensor System raised the expectation that NOBA would be an excellent substrate for CYP102A1 since the oxygen consumption rate with NOBA was even higher than with the natural fatty acid substrates of CYP102A1. This result was, however, not supported by NADPH consumption assays. Oxygen consumption rates for NOBA were apparently six times higher than those for HBA, whereas NADPH consumption rates were less than double. The coupling efficiency for NADPH was also only 57% for NOBA, while it was 77% for HBA. The poor NADPH coupling efficiency observed with NOBA indicates that oxygen consumption will also be uncoupled, but does not completely explain the disproportionately high oxygen consumption observed with NOBA. These results, however, indicate that P450 substrate screening results obtained with fluorescence-based oxygen sensors should be treated with caution and further assays to confirm positive results are essential.

Comparison of the binding constants of CYP102A1 for HBA and NOBA with those for other substrates (Table 1) indicates that CYP102A1 has a higher affinity for HBA and NOBA than for its natural fatty acid substrates such as lauric acid, myristic acid, and palmitic acid as well as other non-natural CYP102A1 substrates such as propylbenzene and branched-chain alcohols and acids. However, despite the fact that HBA and NOBA bind quite strongly to CYP102A1, turnover numbers and coupling efficiencies are much lower than observed with fatty acids and even lower than with propylbenzene (Table 1).

The regioselectivity of hydroxylation of HBA and NOBA by CYP102A1 is very similar to the results obtained with fatty acids. The hydroxylation of HBA was relatively selective, with a constant ratio of 7:1 for the ω−2 and ω−1 positions. Since HBA is also a 13-carbon organic acid, it is remarkable that whole cells of *E. coli* expressing CYP102A1 preferentially hydroxylated tridecanoic acid at the ω−2 position, with an ω−1:ω−2:ω−3 ratio of 1:8:2 (Schneider et al. 1998). Whole-cell hydroxylation of lauric acid, myristic acid, and pentadecanoic acid, on the other hand, occurred at the ω−1, ω−2, and ω−3 positions with almost equal efficiencies, with ω−1:ω−2:ω−3 ratios of 4:3:3, 5:3:3, and 3:5:2, respectively.

NOBA was initially hydroxylated only at the ω−2 position, but the product was subsequently further hydroxylated at the ω−4 position. Following the consumption of NOBA in ethyl acetate extracts did not give satisfactory results and the products from NOBA were difficult to assay using GC. It is therefore possible that more over-oxidized products were formed from NOBA. More work thus needs to be done to develop improved assays for NOBA and its products. Over-oxidation of C-15 and C-16 fatty acids has also been reported by other groups. Schneider et al. (1999) reported multiple oxidation of pentadecanoic acid in reactions with whole cells and cell-free extracts carried out under high oxygen concentration. Boddupalli et al. (1992) also reported multiple oxidation of palmitic acid by purified CYP102A1, but found that lauric acid and myristic acid, the shorter-chain fatty acids, were not over-oxidized.

Whole-cell biotransformations of fatty acids were extensively studied by Schneider et al. (1998, 1999). CYP102A1 was co-expressed with the fatty acid uptake system from *Pseudomonas oleovorans* in *E. coli* K27, a *fadD* mutant strain which cannot degrade fatty acids and their products via β-oxidation. Using this system, the conversion of pentadecanoic acid with cell-free extracts was approximately 24 times faster than with whole cells. The explanation that was offered for the higher specific rate obtained with cell-free extracts was that the whole-cell conversion may have been limited by the availability of endogenous NADPH or by the transfer of the hydrophobic substrate through the cell membrane. In the current study, we have demonstrated that the whole-cell conversion of HBA could be increased at least five-fold by improving the substrate uptake via increased buffer concentration and the use of a co-solvent system. However, the specific CYP102A1 activity with whole cells was still 2.5 times lower than with cell-free extracts. It was thus shown with HBA that, in the case of CYP102A1 expressed in *E. coli*, substrate transfer into the cell can be a rate-limiting factor, even in the case of substrates for which turnover numbers with isolated enzymes are in the order of only 45 min^{-1}. HBA will be used in further comparative studies to investigate factors limiting P450-catalyzed whole-cell biotransformations of fatty acid type substrates. HBA offers the advantage that studies are not limited to engineered hosts with disrupted β-oxidation.

Acknowledgments Financial support by the University of the Free State, the South African National Research Foundation, and the South African Department of Science and Technology/National Research Foundation Centre of Excellence in Catalysis is gratefully acknowledged. We thank Prof. Vlada B. Urlacher for providing the pET28a-*CYP102A1* plasmid, as well as Prof. J. Albertyn and Dr. K. Syed for assistance with transformation into *E. coli*. We also thank Sarel Marais for technical assistance and Charlene Randall for assisting in the preparation of the manuscript.

References

Barrow SE, Taylor GW (1987) Gas chromatography and mass spectrometry of eicosanoids. In: Benedetto C, McDonald-Gibson RG, Nigam S, Slater TF (eds) Prostaglandins and related compounds: a practical approach series. IRL, Oxford, pp 99–141

Boddupalli SS, Estabrook RW, Peterson JA (1990) Fatty acid monooxygenation by cytochrome P-450_{BM-3}. J Biol Chem 265:4233–4239

Boddupalli SS, Pramanik BC, Slaughter CA, Estabrook RW, Peterson JA (1992) Fatty acid monooxygenation by P450BM-3: product identification and proposed mechanism for sequential hydroxylation. Arch Biochem Biophys 292:20–28

Budde M, Morr M, Schmid RD, Urlacher VB (2006) Selective hydroxylation of highly branched fatty acids and their derivatives by CYP102A1 from *Bacillus megaterium*. Chembiochem 7:789–794

Choi S-J, Kim M, Kim SI, Jeon J-K (2003) Microplate assay measurement of cytochrome P450–carbon monoxide complexes. J Biochem Mol Biol 36:332–335

Cryle MJ, Matovic NJ, De Voss JJ (2007) The stereochemistry of fatty acid hydroxylation by cytochrome $P450_{BM3}$. Tetrahedron Lett 48:133–136

Eiben S (2007) CYP102A P450 monooxygenases: comparative analysis and construction of cytochrome P450 chimeras. Thesis, University of Stuttgart

Eiben S, Kaysser L, Maurer S, Kühnel K, Urlacher VB, Schmid RD (2006) Preparative use of isolated CYP102 monooxygenases—a critical appraisal. J Biotechnol 124:662–669

Fujii T, Narikawa T, Sumisa F, Arisawa A, Takeda K, Kato J (2006) Production of α, ω-alkanediols using *Escherichia coli* expressing a cytochrome P450 from *Acinetobacter* sp. OC4. Biosci Biotechnol Biochem 70:1379–1385

Graham-Lorence S, Truan G, Peterson JA, Falck JR, Wei S, Helvig C, Capdevila JH (1997) An active site substitution, F87V, converts cytochrome P450 BM-3 into a regio- and stereoselective (14S, 15R)-arachidonic acid epoxygenase. J Biol Chem 272:1127–1135

Girvan HM, Marshall KR, Lawson RJ, Leys D, Joyce MG, Clarkson J, Smith WE, Cheesman MR, Munro AW (2004) Flavocytochrome P450 BM3 mutant A264E undergoes substrate-dependent formation of a novel heme iron ligand set. J Biol Chem 279:23274–23286

Huang W-C, Westlake ACG, Maréchal J-D, Joyce MG, Moody PCE, Roberts GCK (2007) Filling a hole in cytochrome P450 BM3 improves substrate binding and catalytic efficiency. J Mol Biol 373:633–651

Li Q-S, Ogawa J, Schmid RD, Shimizu S (2001) Residue size at position 87 of cytochrome P450 BM-3 determines its stereoselectivity in propylbenzene and 3-chlorostyrene oxidation. FEBS Lett 508:249–252

Maurer SC, Kühnel K, Kaysser LA, Eiben S, Schmid RD, Urlacher VB (2005) Catalytic hydroxylation in biphasic systems using CYP102A1 mutants. Adv Synth Catal 347:1090–1098

Modi S, Primrose WU, Boyle JMB, Gibson CF, Lian L-Y, Roberts GCK (1995) NMR studies of substrate binding to cytochrome $P_{450\ BM3}$: comparisons to cytochrome P_{450cam}. Biochemistry 34:8982–8988

Mouri T, Michizoe J, Ichinose H, Kamiya N, Goto M (2006) A recombinant *Escherichia coli* whole cell biocatalyst harbouring a cytochrome P450cam monooxygenase system coupled with enzymatic cofactor regeneration. Appl Microbiol Biotechnol 72:514–520

Narhi LO, Fulco AJ (1982) Phenobarbital induction of a soluble cytochrome P-450-dependent fatty-acid mono-oxygenase in *Bacillus megaterium*. J Biol Chem 257:2147–2150

Noble MA, Miles CS, Chapman SK, Lysek DA, Mackay AC, Reid GA, Hanzlik RP, Munro AW (1999) Roles of key active-site residues in flavocytochrome P450BM3. Biochem J 339:371–379

Olry A, Schneider-Belhaddad F, Heintz D, Werck-Reichhart D (2007) A medium-throughput screening assay to determine catalytic activities of oxygen-consuming enzymes: a new tool for functional characterization of cytochrome P450 and other oxygenases. Plant J 51:331–340

Omura T, Sato R (1964) Carbon monoxide-binding pigment of liver microsomes. J Biol Chem 239:2370–2378

Ost TW, Miles CS, Murdoch J, Cheung Y, Reid GA, Chapman SK, Munro AW (2000) Rational re-design of the substrate binding site of flavocytochrome P450 BM3. FEBS Lett 486:173–177

Pflug S, Richter SM, Urlacher VB (2007) Development of a fed-batch process for the production of the cytochrome P450 monooxygenase CYP102A1 from *Bacillus megaterium* in *E. coli*. J Biotechnol 129:481–488

Ravichandran KG, Boddupalli SS, Hasermann CA, Peterson JA, Deisenhofer J (1993) Crystal structure of hemoprotein domain of P450BM-3, a prototype for microsomal P450's. Science 261:731–736

Rolo AP, Palmeira MC, Cortopassi AG (2009) Biosensor plates detect mitochondrial physiological regulators and mutations in vivo. Anal Biochem 385:176–178

Sambrook J, Fritsch EF, Maniatis T (1989) Molecular cloning: a laboratory manual, 2nd edn. Cold Spring Harbor Laboratory Press, New York

Schneider S, Wubbolts MG, Sanglard D, Witholt B (1998) Biocatalyst engineering by assembly of fatty acid transport and oxidation activities for in vivo application of cytochrome P-450$_{BM-3}$ Monooxygenase. Appl Environ Microbiol 64:3784–3790

Schneider S, Wubbolts MG, Oesterhelt G, Sanglard D, Witholt B (1999) Controlled regioselectivity of fatty acid oxidation by whole cells producing cytochrome P450BM-3 monooxygenase under varied dissolved oxygen concentrations. Biotechnol Bioeng 64:333–341

Smit MS, Mokgoro MM, Setati E, Nicaud JM (2005) α, ω-Dicarboxylic acid accumulation by acyl-CoA oxidase deficient mutants of *Yarrowia lipolytica*. Biotechnol Lett 27:859–864

Sowden RJ, Yasmin S, Rees NH, Bell SG, Wong L-L (2005) Biotransformation of the sesquiterpene (+)-valencene by cytochrome P450cam and P450BM-3. Org Biomol Chem 3:57–64

Tsotsou GE, Cass AEG, Gilardi G (2002) High throughput assay for cytochrome P450 BM3 for screening libraries of substrates and combinatorial mutants. Biosens Bioelectron 17:119–131

Wen LP, Fulco AJ (1987) Cloning of the gene encoding a catalytically self-sufficient cytochrome P-450 fatty acid monooxygenase induced by barbiturates in *Bacillus megaterium* and its functional expression and regulation in heterologous (*Escherichia coli*) and homologous (*Bacillus megaterium*) hosts. J Biol Chem 262:6676–6682

Whitehouse CJC, Bell SG, Tufton HG, Kenny RJP, Ogilvie LCI, Wong L-L (2008a) Evolved CYP102A1 (P450BM3) variants oxidise a range of non-natural substrates and offer new selectivity options. Chem Commun 8:966–968

Whitehouse CJC, Bell SG, Wong L-L (2008b) Desaturation of alkylbenzenes by cytochrome P450$_{BM3}$ (CYP102A1). Chem Eur J 14:10905–10908

Whitehouse CJC, Bell SG, Yang W, Yorke JA, Blanford CF, Strong AJF, Morse EJ, Bartlam M, Rao Z, Wong LL (2009) A highly active single-mutation variant of P450BM3 (CYP102A1). Chembiochem 10:1654–1656

Wodnicka M, Guarino RD, Hemperly JJ, Timmins MR, Stitt D, Pitner JB (2000) Novel fluorescent technology platform for high throughput cytotoxicity and proliferation assays. Biomol Screen 5:141–152